Available online at www.sciencedirect.com

ScienceDirect

Procedia IUTAM 12 (2015) 10 – 19

Procedia IUTAM

www.elsevier.com/locate/procedia

IUTAM Symposium on Mechanics of Soft Active Materials

Gel mechanics: A thermo-mechanically coupled theory for fluid permeation in elastomeric materials

Shawn A. Chester[a,*]

[a]*Department of Mechanical $ Industrial Engineering, New Jersey Institute of Technology, Newark, NJ 07102, USA*

Abstract

An elastomeric gel is a cross-linked polymer network swollen with a solvent, and certain gels can undergo large reversible volume changes as they are cycled about a critical temperature. We have developed a continuum-level theory to describe the coupled mechanical deformation, fluid permeation, and heat transfer of such thermally-responsive gels. In discussing special constitutive equations we limit our attention to isotropic materials, and consider a model based on a Flory-Huggins model for the free energy change due to mixing of the fluid with the polymer network, coupled with a non-Gaussian statistical-mechanical model for the change in configurational entropy — a model which accounts for the limited extensibility of polymer chains. We have numerically implemented our theory in a finite element program. We have shown that our theory is capable of simulating swelling, squeezing of fluid by applied mechanical forces, and thermally-responsive swelling/deswelling of such materials.

Peer-review under responsibility of Konstantin Volokh and Mahmood Jabareen.

Keywords: Gels, Elastomeric materials, Diffusion, Large deformations, Thermodynamics

1. Introduction

There are numerous elastomeric materials which can absorb large quantities of various solvents without disrupting the underlying polymeric network structure of the elastomer. Such a polymer network, together with the fluid molecules, forms a swollen aggregate called a *gel*. In this work we restrict our attention to elastomeric gels, and within this class of materials we further restrict our attention to *non-ionic* gels. A subclass of elastomeric gels is known to be *thermally-responsive* — a prime example being gels based on poly(N-isopropylacrylamide), often abbreviated as PNIPAM. An unconstrained specimen of a PNIPAM gel, saturated with an aqueous solution, swells by as much as a factor of 10 when the temperature decreases from above a "critical temperature" to below it. Such a critical temperature for a thermally-responsive gel is known as the the gel's *lower critical solution temperature* (LCST) cf., e.g., Schild [1],Wang et al. [2]. For PNIPAM-based gels the LCST depends on the precise composition of the gel, and may be varied between 30°C to 50°C by suitably varying the composition. PNIPAM-based thermally-responsive gels have been used for a variety of applications including drug delivery [3] and valves in microfluidic devices [4,2], and they show promise for use in a variety of other emerging microscale applications.

* Corresponding author. Tel.: +1-973-596-3658 ; fax: +1-973-642-4282.
E-mail address: shawn.a.chester@njit.edu

Peer-review under responsibility of Konstantin Volokh and Mahmood Jabareen.
doi:10.1016/j.piutam.2014.12.003

Modeling elastomeric gels is interesting and challenging — it involves concurrent deformation of the polymer network and diffusion of the solvent through the network. Early studies of swelling of gels are due to Tanaka and co-workers[5], and in recent years there have been several notable attempts to formulate a coupled deformation-diffusion theory for describing more complete aspects of the response of gels, including swelling and drying, squeezing of fluid by applied mechanical deformation, and forced permeation; cf., e.g., Durning and Morman[6],Srinivasa and Baek[7],Ji et al.[8],Hong et al.[9],Doi[10],Duda et al.[11],Baek and Pence[12]; and references to the vast literature therein. We have recently published a theory for elastomeric gels[13], thermally-responsive elastomeric gels[14], and visco-elastic gels[15].

The work presented here — which is based on a presentation at the IUTAM Symposium on Soft Active Materials — overviews our recent contributions toward modeling and numerically simulating the coupled material behavior of elastomeric gels.

2. Summary of our theory for gels

In this section we briefly summarize the basic continuum mechanical theory for thermally responsive elastomeric gels. In what follows we neglect thermal expansion/contraction effects since they are small compared to the large volume changes observed due to swelling/deswelling. Cf. Chester and Anand[14] for complete details of the formulation of the theory.

2.1. Kinematics. Constitutive theory

Consider a fluid-free (dry) macroscopically homogeneous elastomeric body. We identify such a macroscopically-homogeneous body B with the region of space it occupies in a fixed reference configuration, and denote by $\mathbf{X}$ an arbitrary material point of B. A motion of B is then a smooth one-to-one mapping $\mathbf{x} = \boldsymbol{\chi}(\mathbf{X}, t)$ with deformation gradient, velocity, and velocity gradient given by[1]

$$\mathbf{F} = \nabla\boldsymbol{\chi}, \qquad \mathbf{v} = \dot{\boldsymbol{\chi}}, \qquad \mathbf{L} = \operatorname{grad}\mathbf{v} = \dot{\mathbf{F}}\mathbf{F}^{-1}. \tag{1}$$

The deformed body is denoted as $\mathcal{B}$.

The theory is based upon a multiplicative decomposition

$$\mathbf{F} = \mathbf{F}^e\mathbf{F}^s, \qquad \text{with} \qquad \mathbf{F}^s = \lambda^s\mathbf{1}, \qquad \lambda^s > 0, \tag{2}$$

of the deformation gradient $\mathbf{F}$ into elastic and swelling parts $\mathbf{F}^e$ and $\mathbf{F}^s$, respectively, with the swelling taken to be isotropic, where λ^s is the swelling stretch. With Ω denoting the volume of a mole of fluid molecules, we assume the swelling stretch is given by

$$\lambda^s = (1 + \Omega c_{\text{R}})^{1/3}, \tag{3}$$

where c_{R} represents the *fluid concentration* measured in moles of fluid per unit reference volume of the dry elastomer.

The constitutive equations of the theory are:

- **Free energy**: A simple form of the free energy function which accounts for the combined effects of mixing, swelling, and elastic stretching is,

$$\begin{aligned}\psi_{\text{R}} = {}& \mu^0 c_{\text{R}} + R\vartheta c_{\text{R}}\left(\ln\left(\frac{\Omega c_{\text{R}}}{1+\Omega c_{\text{R}}}\right) + \chi\left(\frac{1}{1+\Omega c_{\text{R}}}\right)\right) \\ & + G_0\lambda_L^2\left[\left(\frac{\bar{\lambda}}{\lambda_L}\right)\beta + \ln\left(\frac{\beta}{\sinh\beta}\right) - \left(\frac{1}{\lambda_L}\right) - \ln\left(\frac{\beta_0}{\sinh\beta_0}\right)\right] - G_0\left(\frac{\lambda_L}{3}\right)\beta_0\ln J + J^s\left[\tfrac{1}{2}K(\ln J^e)^2\right] + f(\vartheta).\end{aligned} \tag{4}$$

[1] Notation: We use standard notation of modern continuum mechanics[16]. Specifically: ∇ and Div denote the gradient and divergence with respect to the material point $\mathbf{X}$ in the reference configuration; grad and div denote these operators with respect to the point $\mathbf{x} = \boldsymbol{\chi}(\mathbf{X}, t)$ in the deformed body; a superposed dot denotes the material time-derivative. Throughout, we write $\mathbf{F}^{e-1} = (\mathbf{F}^e)^{-1}$, $\mathbf{F}^{e-\top} = (\mathbf{F}^e)^{-\top}$, etc. We write $\operatorname{tr}\mathbf{A}$, $\operatorname{sym}\mathbf{A}$, $\operatorname{skw}\mathbf{A}$, $\mathbf{A}_0$, and $\operatorname{sym}_0\mathbf{A}$ respectively, for the trace, symmetric, skew, deviatoric, and symmetric-deviatoric parts of a tensor $\mathbf{A}$. Also, the inner product of tensors $\mathbf{A}$ and $\mathbf{B}$ is denoted by $\mathbf{A}:\mathbf{B}$, and the magnitude of $\mathbf{A}$ by $|\mathbf{A}| = \sqrt{\mathbf{A}:\mathbf{A}}$.

Here, μ^0 is a reference chemical potential for the fluid, R the gas constant, ϑ is the current temperature, $\chi(\vartheta)$ is a dimensionless measure of the "enthalpy" of mixing known as the Flory-Huggins interaction parameter, $G_0(\vartheta) = N_{\text{R}} k_B \vartheta$ is the ground state shear modulus of the network with N_{R} the number of polymer chains per reference volume, and k_B the Boltzmann constant, K is a bulk modulus of the gel, and

$$\bar{\lambda} \stackrel{\text{def}}{=} \sqrt{\frac{1}{3}\text{tr}\mathbf{C}} = \sqrt{\frac{1}{3}(1+\Omega c_{\text{R}})^{2/3}\,\text{tr}\mathbf{C}^e}, \tag{5}$$

is an *effective stretch*. Also

$$\beta \stackrel{\text{def}}{=} \mathcal{L}^{-1}\left(\frac{\bar{\lambda}}{\lambda_L}\right), \quad \text{and} \quad \beta_0 \stackrel{\text{def}}{=} \mathcal{L}^{-1}\left(\frac{1}{\lambda_L}\right) \tag{6}$$

where $\mathcal{L}^{-1}$ is the inverse of the Langevin function $\mathcal{L}(x) = \coth(x) - 1/x$. The term $f(\vartheta)$ is related to the specific heat of the material and we leave it unspecified here. Next, we specialize the temperature dependence of the chi-parameter $\chi(\vartheta)$ in the Flory-Huggins expression (4) for the free energy of mixing. Recall that this parameter represents the dis-affinity between the polymer and the solvent — if $\chi(\vartheta)$ is increased, the fluid molecules are expelled from the gel and the gel shrinks, while if $\chi(\vartheta)$ is decreased, the gel absorbs more fluid and swells. As reviewed elsewhere, thermally-responsive gels possess a critical transition temperature, ϑ_T, and exhibit a larger degree of swelling at temperatures below ϑ_T than at temperatures above ϑ_T Gotoh et al. e.g.,[17],Afroze et al. e.g.,[18],Xue et al. e.g.,[19],Zhang et al. e.g.,[20],Liu et al. e.g.,[21]. To model such experimentally-observed phenomena we assume that

$$\chi(\vartheta) = \tfrac{1}{2}(\chi_L + \chi_H) - \tfrac{1}{2}(\chi_L - \chi_H)\tanh\left(\frac{\vartheta - \vartheta_T}{\Delta}\right) \tag{7}$$

where ϑ_T is the transition temperature of the gel, χ_L is the value of $\chi(\vartheta)$ below the transition temperature, $\chi_H > \chi_L$ is the value of $\chi(\vartheta)$ above the transition temperature, with Δ the width of the transition in temperatures between χ_L and χ_H.

- **Constitutive equation for the Cauchy stress**: Corresponding to the free energy (4), the Cauchy stress $\mathbf{T}$ is given by

$$\mathbf{T} = J^{-1}\left(2\mathbf{F}^e\frac{\partial\psi_{\text{R}}}{\partial\mathbf{C}^e}\mathbf{F}^{e\text{T}}\right) = J^{-1}\left[G_0\,\zeta\phi^{-2/3}\mathbf{B}^e - G_0\zeta_0\mathbf{1} + J^s K(\ln J^e)\mathbf{1}\right], \tag{8}$$

where we have introduced the *polymer volume fraction* defined by

$$\phi \stackrel{\text{def}}{=} \frac{1}{1+\Omega c_{\text{R}}} = (\lambda^s)^{-3}, \tag{9}$$

and the terms

$$\zeta \stackrel{\text{def}}{=} \left(\frac{\lambda_L}{3\bar{\lambda}}\right)\mathcal{L}^{-1}\left(\frac{\bar{\lambda}}{\lambda_L}\right), \quad \text{and} \quad \zeta_0 \stackrel{\text{def}}{=} \left(\frac{\lambda_L}{3}\right)\mathcal{L}^{-1}\left(\frac{1}{\lambda_L}\right) \tag{10}$$

Next, since

$$\mathbf{B}(\equiv \mathbf{F}\mathbf{F}^{\text{T}}) = (\lambda^s)^2\mathbf{B}^e = \phi^{-2/3}\mathbf{B}^e, \tag{11}$$

(8) reduces to

$$\mathbf{T} = J^{-1}\left[G_0\,(\zeta\mathbf{B} - \zeta_0\mathbf{1}) + J^s K(\ln J^e)\mathbf{1}\right]. \tag{12}$$

- **Constitutive equation for the chemical potential**: The chemical potential μ is given by

$$\mu = \frac{\partial\psi_{\text{R}}}{\partial c_{\text{R}}} - \Omega\frac{1}{3}J^e\text{tr}\mathbf{T} = \mu^0 + R\vartheta\Big(\ln(1-\phi) + \phi + \chi\phi^2\Big) - \Omega K(\ln J^e) + \tfrac{1}{2}K\Omega(\ln J^e)^2. \tag{13}$$

- **Constitutive equation for the fluid flux**: We assume that the spatial fluid flux, $\mathbf{j}$, depends linearly on the spatial gradient of the chemical potential, $\text{grad}\,\mu$, with the mobility tensor taken to be isotropic so that

$$\mathbf{j} = -m\,\text{grad}\,\mu, \tag{14}$$

where m is a scalar mobility coefficient, which in general is an isotropic function of the stretch and the fluid concentration. In what follows, we assume here that the mobility is given by

$$m = \frac{Dc}{R\vartheta}, \tag{15}$$

where $D > 0$, a constant, represents a diffusion coefficient, and $c = c_{\mathrm{R}}/J$ is the fluid concentration measured in moles of fluid per unit deformed volume.

- **Constitutive equation for the heat flux**: We assume that the spatial heat flux, $\mathbf{q}$, depends linearly on the spatial gradient of the temperature, $\operatorname{grad}\vartheta$, with the thermal conductivity tensor taken to be isotropic so that

$$\mathbf{q} = -k \operatorname{grad}\vartheta, \tag{16}$$

where k is the scalar thermal conductivity, which in general is an isotropic function of the stretch and the fluid concentration.

2.2. Governing partial differential equations

The governing partial differential equations, when expressed in the deformed body, consist of

1. The local force balance for the macroscopic Cauchy stress,

$$\operatorname{div}\mathbf{T} + \mathbf{b} = \mathbf{0}, \tag{17}$$

with $\mathbf{b}$ a non-inertial body force, and $\mathbf{T}$ given by (12).

2. The local balance for the fluid concentration,

$$\dot{c}_{\mathrm{R}} = -J\operatorname{div}\mathbf{j}, \tag{18}$$

which using (9) may be written in the form

$$\frac{\dot{\phi}}{J\Omega\phi^2} - \operatorname{div}\mathbf{j} = 0, \tag{19}$$

in which the fluid flux $\mathbf{j}$ is given by (14), and the chemical potential μ is given by (13).

3. The local energy balance for the temperature,

$$c\dot{\vartheta} + \operatorname{div}\mathbf{q} = h \tag{20}$$

where h is the contribution due to any source/sink terms, and the heat flux $\mathbf{q}$ is given by (16).

2.3. Boundary and initial conditions

We also need boundary and initial conditions to complete the theory. Let $\mathcal{S}_{\mathbf{u}}$ and $\mathcal{S}_{\mathbf{t}}$ be complementary subsurfaces of the boundary $\partial\mathcal{B}$ of the body $\mathcal{B}$ in the sense $\partial\mathcal{B} = \mathcal{S}_{\mathbf{u}} \cup \mathcal{S}_{\mathbf{t}}$ and $\mathcal{S}_{\mathbf{u}} \cap \mathcal{S}_{\mathbf{t}} = \emptyset$. Similarly let $\mathcal{S}_{\mu}$ and $\mathcal{S}_{\mathbf{j}}$ be complementary subsurfaces of the boundary: $\partial\mathcal{B} = \mathcal{S}_{\mu} \cup \mathcal{S}_{\mathbf{j}}$ and $\mathcal{S}_{\mu} \cap \mathcal{S}_{\mathbf{j}} = \emptyset$. And lastly let $\mathcal{S}_{\vartheta}$ and $\mathcal{S}_{\mathbf{q}}$ be complementary subsurfaces of the boundary: $\partial\mathcal{B} = \mathcal{S}_{\vartheta} \cup \mathcal{S}_{\mathbf{q}}$ and $\mathcal{S}_{\vartheta} \cap \mathcal{S}_{\mathbf{q}} = \emptyset$. Then for a time interval $t \in [0, T]$ we consider a pair of boundary conditions in which the displacement $\mathbf{u}$ is specified on $\mathcal{S}_{\mathbf{u}}$ and the surface traction on $\mathcal{S}_{\mathbf{t}}$:

$$\left.\begin{aligned} \mathbf{u} &= \breve{\mathbf{u}} \quad \text{on } \mathcal{S}_{\mathbf{u}} \times [0, T], \\ \mathbf{T}\mathbf{n} &= \breve{\mathbf{t}} \quad \text{on } \mathcal{S}_{\mathbf{t}} \times [0, T]; \end{aligned}\right\} \tag{21}$$

and a pair of boundary conditions in which the chemical potential is specified on $\mathcal{S}_{\mu}$ and the fluid flux on $\mathcal{S}_{\mathbf{j}}$

$$\left.\begin{aligned} \mu &= \breve{\mu} \quad \text{on } \mathcal{S}_{\mu} \times [0, T], \\ -\mathbf{j} \cdot \mathbf{n} &= \breve{j} \quad \text{on } \mathcal{S}_{\mathbf{j}} \times [0, T]; \end{aligned}\right\} \tag{22}$$

and a pair of boundary conditions in which the temperature is specified on $\mathcal{S}_\vartheta$ and the heat flux on $\mathcal{S}_\mathbf{q}$

$$\left.\begin{aligned} \vartheta &= \breve{\vartheta} \quad \text{on } \mathcal{S}_\vartheta \times [0,T], \\ -\mathbf{q}\cdot\mathbf{n} &= \breve{q} \quad \text{on } \mathcal{S}_\mathbf{q} \times [0,T]; \end{aligned}\right\} \tag{23}$$

with $\breve{\mathbf{u}}$, $\breve{\mathbf{t}}$, $\breve{\mu}$, $\breve{j}$, $\breve{\vartheta}$, $\breve{q}$ *prescribed* functions of $\mathbf{x}$ and t. The initial data is taken as

$$\mathbf{u}(\mathbf{X},0) = \mathbf{u}_0(\mathbf{X}), \quad \text{and} \quad \mu(\mathbf{X},0) = \mu_0(\mathbf{X}) \quad \text{and} \quad \vartheta(\mathbf{X},0) = \vartheta_0(\mathbf{X}) \quad \text{in} \quad \mathrm{B}. \tag{24}$$

The coupled set of equations (17), (19), and (20), together with (21), (22), (23), and (24) yield an initial boundary value problem for the displacement $\mathbf{u}(\mathbf{x},t)$, the chemical potential $\mu(\mathbf{x},t)$, and the temperature $\vartheta(\mathbf{x},t)$.

3. Numerical examples

3.1. Material parameters

Table 1 lists plausible representative values for the material properties of a thermally responsive polymeric gel, which we have used in our calculations. Specifically, the ground state shear modulus for the polymer, G, is chosen

Parameter	Value
N_R	2.43×10^{25} /m^3
$G = N_\mathrm{R} k_B \vartheta$ (at 298 K)	0.1 MPa
K	10 MPa
Ω	1.0×10^{-4} m^3/mol
χ_L	0.1
χ_H	0.7
ϑ_T	320 K
Δ	5.0 K
μ^0	0.0 J/mol
D	5×10^{-9} m^2/s
c	4.18×10^6 J/(m^3 K)
k	0.5 W/(m K)

Table 1. Material parameters for a representative thermally responsive elastomeric gel.

to have a value 0.1 MPa at room temperature, and the bulk modulus K is taken to be two orders of magnitude larger. The volume of a solvent molecule is taken as $\Omega = 1.0\times10^{-4}$ m^3/mol, and the reference chemical potential of the fluid is taken as $\mu^0 = 0.0$ J/mol. Additionally, we have chosen values $\chi_L = 0.1$, and $\chi_H = 0.7$, for the Flory-Huggins interaction parameter, with $\vartheta_T = 320$ K and $\Delta = 5.0$ K. As a representative value in our numerical simulations we take $D = 5\times10^{-9}$ m^2/s. And lastly for the thermal properties we assume a constant specific heat per unit volume $c = 4.18\times10^6$ J/(m^3 K) and thermal conductivity $k = 0.5$ W/(m K) .

3.2. Swelling induced three-dimensional buckling of constrained cylindrical tubes

This first example problem is modeled after the recent experiments conducted by Lee et al. [22] on hydrogel tubes. Their experiments consisted of cylindrical tubes of hydrogels which were mechanically constrained on one end, while the other end was placed in contact with a fluid and allowed to swell and possibly buckle. In their experiments Lee et al. [22] varied the geometry of their tubes and found that varying the wall thickness, radii, and heights of their tubes resulted in the formation of different "buckled" patterns to form on the swollen ends of their hydrogel tubes.

Due to the nature of the experimentally-observed three-dimensional buckled patterns, we model the body in three dimensions. Fig. 1 shows the basic geometry under consideration, a tube with outer diameter D_0, wall thickness t_0, and height H_0 in the initial dry configuration. We consider two initial geometries:

$$\{D_0, t_0, H_0\} = \{4.636, 0.206, 0.6\}\,\mathrm{mm} \quad \text{and} \quad \{4.636, 0.309, 1.2\}\,\mathrm{mm}$$

for our numerical simulations. These dimensions were chosen to provide two distinct swollen shapes similar to those reported in the recent paper of Lee et al. [22]. Guided by the (approximate) symmetry observed in their experiments, we model only 1/4 of the geometry. The initial meshes are shown in Fig. 1, they consist of 2720, and 6840 8-node brick elements with 4 and 6 elements through the thickness for the "short" and "tall" geometries, respectively. In order to aid the initiation of buckling, all nodes on the front face of the cylindrical body were given a small random geometric imperfection on the order 10^{-2} mm times a random number in the height dimension.

The initial condition for the chemical potential of the dry swellable gel is taken to be $\mu(\mathbf{X}, t = 0) = \mu_0 = -14388.57$ J/mole (computed from (13)). For the mechanical boundary conditions, referring to Fig. 1, we assume that the back face is held fixed, all symmetry planes are prescribed appropriate symmetry conditions, and the remaining faces are traction free. For the chemical boundary conditions, we assume that only the front face is in contact with the fluid, and prescribe $\breve{\mu}(t) = \mu^0 + \mu_0 \exp(-t/t_d)$ with $t_d = 300$ s while all other faces are flux free.

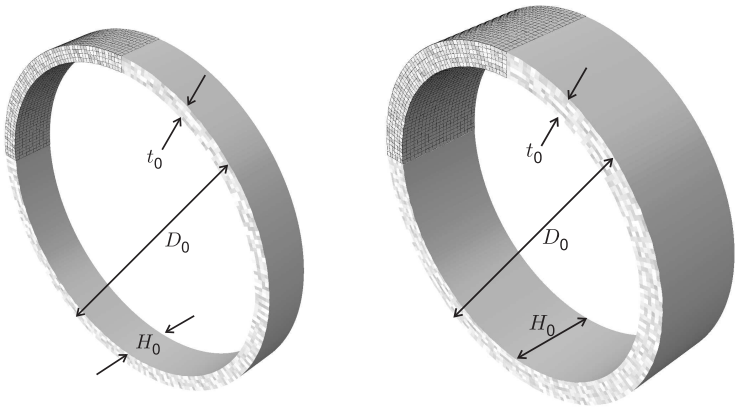

Fig. 1. Initial geometries used in the swell induced buckling simulations. Only one-quarter of the geometry is meshed and symmetry boundary conditions are assumed.

Fig. 2 shows contours of the polymer volume fraction on the deformation body after 215s, 250s, and 900s, for (a) the "short-thin" tube and (b) the "tall-thick" tube. These shapes resemble those observed experimental by Lee et al. [22], and we note that the initial geometry in Fig. 2(a) results in a "buckled" pattern, while the initial geometry in Fig. 2(b) results in an axisymetrically swollen tube. These simulation results show that our three-dimensional model and numerical implementation are able to capture the differing deformed shapes in the two geometries due to swelling.

3.3. Thermally-actuated valves

In a classical paper, Beebe et al. [23] have experimentally demonstrated the use of hydrogels for applications as valves in microfluidic devices. Here, following the ideas of Beebe et al. we simulate the essential features of their experiments using our model for thermally-responsive hydrogels; a schematic of the geometry under consideration is shown in Figure 3. The geometry consists of three cylindrical pillars of a thermally-responsive elastomeric gel, each of initial diameter $20\,\mu$m, inside a fluid-containing channel of width $H_0 = 120\,\mu$m; the centers of the gel pillars are fixed in place. Due to the symmetry of the problem, we model only the upper quarter of the geometry which is indicated by the solid black-filled region in Figure 3a. The initial finite element mesh is shown in Figure 3b; it consists of 62 4-node quadrilateral elements.

The simulation is carried out in three steps:

1. In the first step, the fluid is allowed to diffuse into the dry gel at a constant fluid temperature of ϑ=298 K for 0.85 seconds. This causes the gel pillars to increase in diameter and contact with each other and the walls of the channel, and thereby to seal-off one side of the channel from the other.

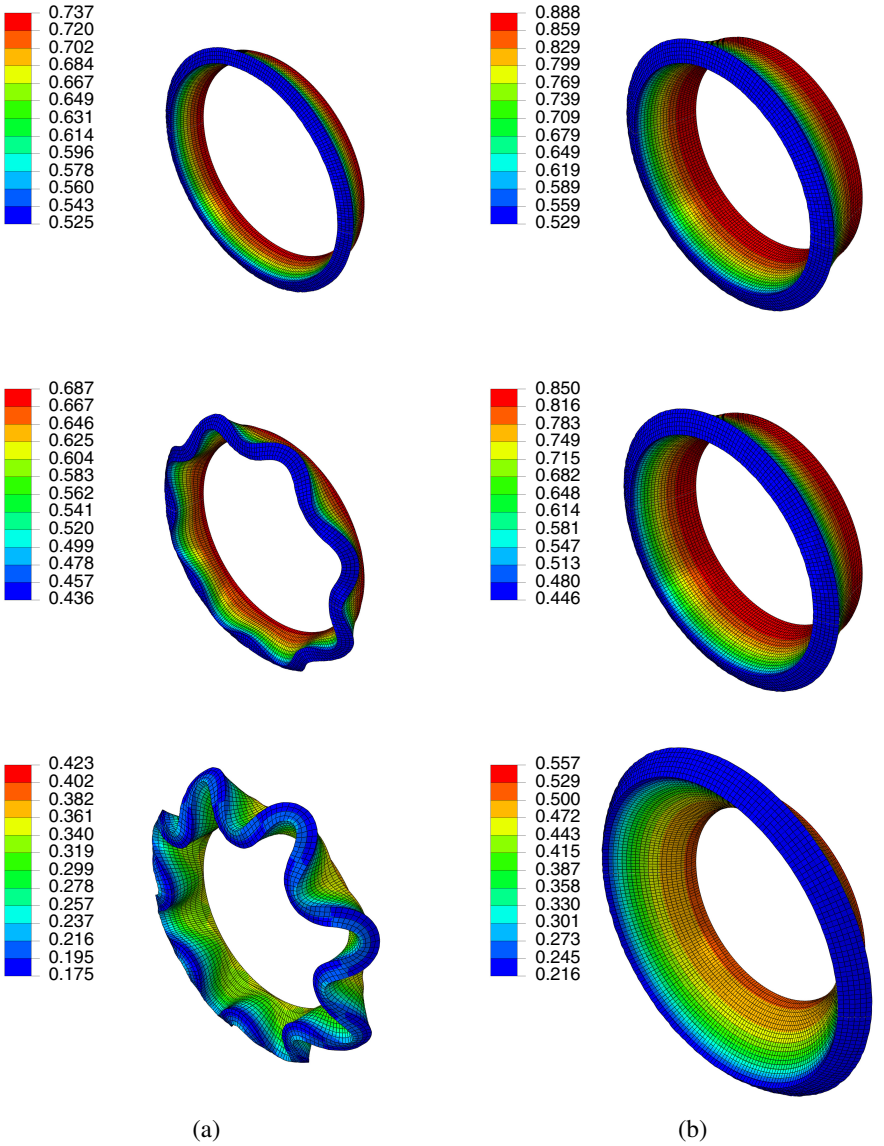

Fig. 2. Contours of the polymer volume fraction ϕ on the deformed body for $\{D_0, t_0, H_0\}$ given by (a) $\{4.636, 0.206, 0.6\}$ mm and (b) $\{4.636, 0.361, 1.825\}$ mm, at 215 s (top), 250 s (middle), and 900 s (bottom) of swelling. Note how the initial geometry leads to very different swollen shapes, one buckled and the other stable.

2. In the second step, the temperature of the fluid is raised from 298 K to 333 K (which is above its critical transition temperature $\vartheta_T = 320$ K) over a period of 0.25 seconds, and the temperature is then held constant for another 0.6 seconds. This temperature rise causes the gel pillars to shrink in diameter, and the gel-based valve is opened.
3. In the third step, the temperature of the fluid is decreased from 333 K to 298 K over a period of 0.25 seconds, and the temperature is then held constant for another 0.6 seconds. This temperature decrease causes the gel pillars to grow in diameter, and the gel-based valve is once again closed.

Referring to Figure 3b, the boundary conditions used in the simulation are as follows:

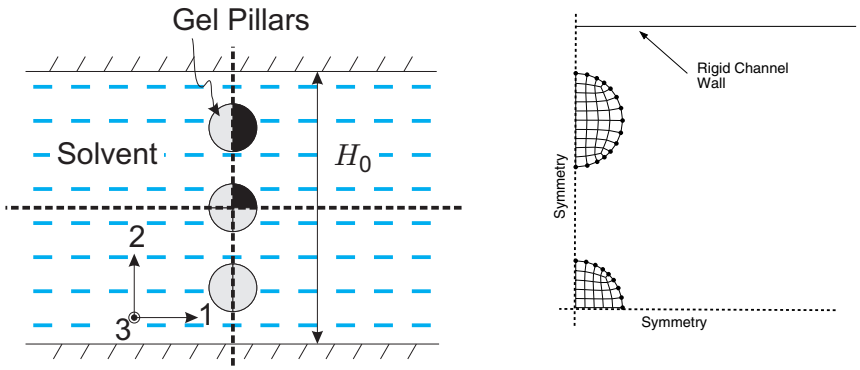

Fig. 3. (a) Schematic of the geometry for the gel-based fluidic-valve. The thick dashed-lines indicate the symmetry lines; the finite element calculation is performed only for the top right quarter of the body shown in black. (b) Finite element mesh of the gel-based fluidic-valve example. The dashed-lines indicate the symmetry planes.

- For the mechanical boundary conditions, the nodes along the vertical symmetry line are prescribed $u_1 = 0$, while the nodes along the horizontal symmetry line are prescribed $u_2 = 0$. The valve-valve and the valve-wall contact is modeled as frictional with a Coulomb coefficient of friction of 0.7.
- For the thermal boundary conditions, the edges along the symmetry lines are prescribed zero heat flux, whereas the highlighted outer nodes are prescribed the fluid temperature as described in the prior paragraph.
- For the chemical boundary conditions, the edges along the symmetry lines are prescribed zero fluid flux. The highlighted outer nodes are prescribed a chemical potential $\breve{\mu}(t) = \mu^0$.

Regarding the initial conditions, the gel valves are taken to be stress free, at a temperature $\vartheta_0 = 298\,\mathrm{K}$, and a chemical potential $\mu_0 = -14388.57\,\mathrm{J/mole}$.

Figure 4 shows the gel valves and contours of the polymer volume fraction, ϕ: (a) at the end of the first swelling step; (b) at the end of the second heating step; and (c) at the end of the third cooling step. In this figure, for clarity of presentation, we have removed the channel walls, mirrored the geometry of the valves about symmetry planes, and extruded the plane-strain elements. The thick dashed-lines indicate the original cylindrical dry polymer pillars before swelling. The length scale is the same for all sub-figures; however, note the change in scale for the contours of polymer volume fraction in each subfigure.

Additionally, Figure 5 shows the force exerted onto the upper rigid channel wall during operation of the microvalve. The valve is "open" at times when the gel is not in contact with the channel wall (zero force), and that the valve is closed when the gel is in contact with the channel wall (non-zero force). Since actuation is diffusion limited, this figure also serves to show the extremely quick response time for swelling and deswelling of this micro-scale device when compared to the previous macro-scale simulation — seconds compared to minutes.

4. Concluding remarks

We have reviewed the thermodynamically consistent continuum-mechanical theory developed in Chester and Anand [14] to describe the coupled heat transfer, fluid permeation, and large deformation behavior of thermally responsive neutral elastomeric gels. The coupled theory was implemented as a user-defined element (UEL) subroutine in Abaqus/Standard [24]. We have shown the robustness of the theory and it's numerical implementation via a handful of simulations that explore physically interesting and technologically important problems. However, much work remains to be done in terms of experiments and validation of the theory.

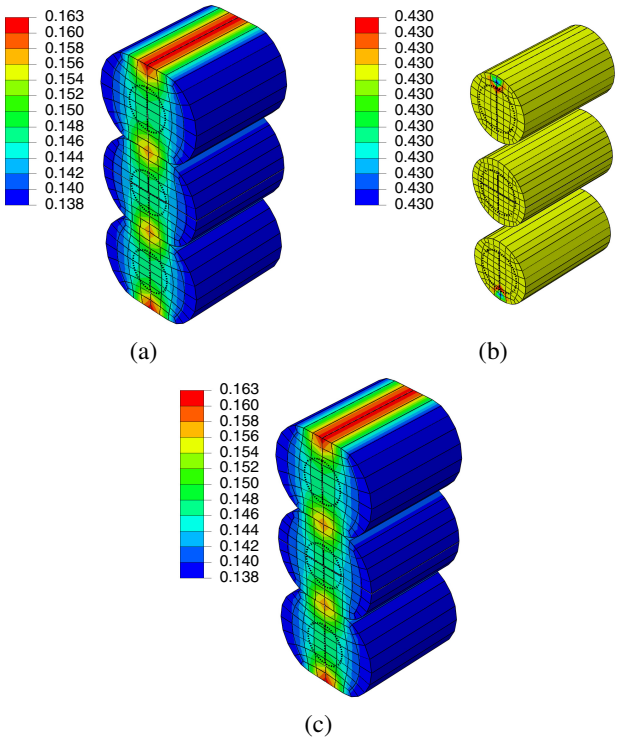

Fig. 4. Geometry of the gel-pillar and contours of the polymer volume fraction, ϕ: (a) at the end of the swelling step; (b) at the end of the heating step; and (c) at the end of the cooling step. The thick dashed-lines indicate the original body before swelling. The length scale is the same for all sub-figures; however, note the change in scale for the contours of ϕ for each time.

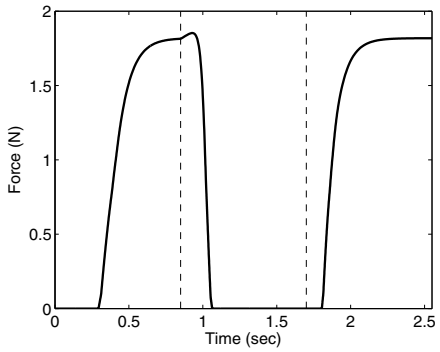

Fig. 5. Force per unit depth that the gel valves exert on the upper rigid channel wall. The valve is "open" when the gel is not in contact with the channel wall (zero force), and the valve is closed when the gel is in contact with the channel wall (non-zero force). The vertical dashed lines split the curve corresponding to the initial swelling, heating, and then cooling steps as described in Section 3.3. The slight peak just at the start of the heating step is due to the initial increase of the shear modulus with temperature.

Acknowledgements

The author sincerely thanks Professor Konstantin Volokh and colleagues at Technion for organizing the IUTAM Symposium on Mechanics of Soft Active Materials Symposium.

References

1. Schild, H.. Poly (n-isopropylacrylamide): experiment, theory, and application. *Progress in Polymer Science* 1992;**17**:163–249.
2. Wang, J., Chen, Z., Mauk, M., Hong, K., Li, M., Yang, S., et al. Self-actuated, thermo-responsive hydrogel valves for lab on a chip. *Biomedical Microdevices* 2005;**7**:313–322.
3. Dinarvand, R., D'Emanuele, A.. The use of thermoresponsive hydrogels for on-off release of molecules. *Journal of Controlled Release* 1995;**36**:221–227.
4. Harmon, M., Tang, M., Frank, C.. A microfluidic actuator based on thermoresponsive hydrogels. *Polymer* 2003;**44**:4547–4556.
5. Tanaka, T., Fillmore, D.. Kinetics of swelling of gels. *Journal of Chemical Physics* 1979;**70**:1214–1218.
6. Durning, C., Morman, K.. Nonlinear swelling of polymer gels. *Journal of Chemical Physics* 1993;**98**:4275–4293.
7. Srinivasa, A., Baek, S.. Diffusion through an elastic solid undergoing large deformation. *Journal of Non-Linear Mechanics* 2004;**39**:201–218.
8. Ji, H., Mourad, H., Fried, E., Dolbow, J.. Kinetics of thermally induced swelling of hydrogels. *International Journal of Solids and Structures* 2005;**43**:1878–1907.
9. Hong, W., Zhao, X., Zhou, J., Suo, Z.. A theory of coupled diffusion and large deformation in polymeric gels. *Journal of the Mechanics and Physics of Solids* 2008;**56**(5):1779 – 1793.
10. Doi, M.. Gel dynamics. *Journal of the Physical Society of Japan* 2009;**78**:052001.
11. Duda, F.P., Souza, A.C., Fried, E.. A theory for species migration in a finitely strained solid with application to polymer network swelling. *Journal of the Mechanics and Physics of Solids* 2010;**58**(4):515 – 529. URL: `http://www.sciencedirect.com/science/article/pii/S0022509610000189`. doi:http://dx.doi.org/10.1016/j.jmps.2010.01.009.
12. Baek, S., Pence, T.. Inhomogeneous deformation of elastomer gels in equilibrium under saturated and unsaturated conditions. *Journal of the Mechanics and Physics of Solids* 2011;**59**:561–582.
13. Chester, S.A., Anand, L.. A coupled theory of fluid permeation and large deformations for elastomeric materials. *Journal of the Mechanics and Physics of Solids* 2010;**58**(11):1879 – 1906.
14. Chester, S.A., Anand, L.. A thermo-mechanically coupled theory for fluid permeation in elastomeric materials: Application to thermally responsive gels. *Journal of the Mechanics and Physics of Solids* 2011;**59**(10):1978 – 2006.
15. Chester, S.. A constitutive model for coupled fluid permeation and large viscoelastic deformation in polymeric gels. *Soft Matter* 2012; **8**:8223–8233.
16. Gurtin, M., Fried, E., Anand, L.. *The Mechanics and Thermodynamics of Continua*. Cambridge University Press; 2010.
17. Gotoh, T., Nakatani, Y., Sakohara, S.. Novel synhesis of thermosensitive porous hydrogels. *Journal of Applied Polymer Science* 1998; **69**:895–906.
18. Afroze, F., Nies, E., Berghmans, H.. Phase transitions in the system poly(n-isopropylacrylamide)/water and swelling behavior of the corresponding networks. *Journal of Molecular Structure* 2000;**554**:5568.
19. Xue, W., Champ, S., Huglin, M.. New superabsorbant thermo reversable hydrogels. *Polymer* 2001;**42**:2247–2250.
20. Zhang, X., Wang, F., Chu, C.. Thermoresponsive hydrogel with rapid response dynamics. *Journal of Materials Science: Materials in Medicine* 2003;**14**:451–455.
21. Liu, K., Ovaert, T., Mason, J.. Preparation and mechanical characterization of a pnipa hydrogel composite. *Journal of Materials Science: Materials in Medicine* 2008;**19**:1815–1821.
22. Lee, H., Zhang, J., Jiang, H., Fang, N.X.. Prescribed pattern transformation in swelling gel tubes by elastic instability. *Phys Rev Lett* 2012; **108**:214304. URL: `http://link.aps.org/doi/10.1103/PhysRevLett.108.214304`. doi:10.1103/PhysRevLett.108.214304.
23. Beebe, D., Moore, J., Auer, J., Yu, Q., Liu, R., Devadoss, C., et al. Functional hydrogel structures for autonomous flow control inside microfluidic devices. *Nature* 2000;**404**:588–590.
24. Abaqus/standard, simulia. 2014.